

Technical Note

Prosthetic Heart Valves: Evaluation of Magnetic Field Interactions, Heating, and Artifacts at 1.5 T

Maria-Benedicta Edwards, MPhil,¹ Kenneth M. Taylor, FRCS,¹ and Frank G. Shellock, PhD^{2*}

The purpose of this study was to use ex vivo testing techniques to determine the magnetic resonance imaging (MRI) safety aspects for 32 different heart valve prostheses that had not been evaluated previously in association with the 1.5-T MR environment. Ex vivo testing was performed using previously described techniques for the evaluation of magnetic field interactions (deflection angle and torque), heating [gel-filled phantom and fluoroptic thermometry; 15 minutes of MRI at a specific absorption rate (SAR) of 1.1 W/kg], and artifacts (using gradient echo and T1-weighted spin-echo pulse sequences). Thirteen heart valve prostheses displayed interactions with the magnetic field. However, these magnetic field interactions were considered relatively minor. Heating was $\leq 0.8^{\circ}\text{C}$ for these implants. Artifacts varied from mild to severe depending on the amount and type of metal used to make the particular heart valve prosthesis. For these 32 different heart valve prostheses, the relative lack of substantial magnetic field interactions and negligible heating indicate that MR procedures may be conducted safely in individuals with these implants using MR systems with static magnetic fields of 1.5 T or less. *J. Magn. Reson. Imaging* 2000;12:363–369. © 2000 Wiley-Liss, Inc.

Index terms: magnetic resonance imaging, safety; magnetic resonance imaging, bioeffects; heart valve prostheses; implants; heating; artifacts

MRI of patients with biomedical implants continues to be a major concern for MR health care workers. Notably, MRI may be contraindicated for patients with ferromagnetic bioimplants because of the relative risks related to the possible dislodgment of the implant or substantial heating of the device in association with an MR procedure (1–30). The induction of an electrical current may also present possible hazards, but this does not appear to be problematic for passive implants (ie, those that do not operate by means of electrical power) (5,6,8). Despite these concerns, research has

shown that many metallic implants are generally safe for patients undergoing MR procedures if they are non-ferromagnetic or, if the magnetic attraction of the implant is less than the force applied compared with the in vivo application of the implant (2,6–27,29,30).

There are many different types of heart valve prostheses used in patients today. However, relatively little published information exists regarding MRI safety for many of the heart valves currently used in patients throughout the world (26–31). Therefore, the main objective of this research study was to determine the MRI safety for 32 different heart valve prostheses using ex vivo techniques to assess magnetic field interactions and heating. Additionally, artifacts were characterized for these implants.

MATERIALS AND METHODS

Heart Valve Prostheses

Thirty-two different heart valve prostheses were evaluated for MR safety. These implants were primarily selected for evaluation because of the lack of safety information relative to the 1.5-T MR environment. In addition, inclusion based on registration of the heart valve prosthesis in the comprehensive listing of the UK Heart Valve Registry database and the volume of requests received by the Registry for information on MRI safety for the specific heart valve prostheses (31). Details for the prosthetic heart valve prostheses evaluated in the study are shown in Table 1.

Assessment of Magnetic Field Interactions

An assessment of magnetic field translational attraction was performed on each heart valve prosthesis. This test was conducted using a standardized procedure indicated as the deflection angle test (2,15,24,29,32,33). Each heart valve was suspended by a 30-cm-long piece of lightweight thread that was attached to the estimated center of the device. The thread was then attached to a sturdy plastic protractor so that the angle of deflection from the vertical could be measured. The accuracy of this measuring device is $\pm 0.5^{\circ}$ based on the ability to read the protractor in the MR system. Deflection angles were determined three times for each implant and averaged.

Notably, the deflection angle test was conducted at the position in the shielded 1.5-T MR system where the

This article was originally submitted for publication in the Special Issue on MR Safety which published in June 2000.

¹United Kingdom Heart Valve Registry, Department of Cardiothoracic Surgery, Hammersmith Hospital, Du Cane Road, London W12 0NN, United Kingdom.

²Department of Radiology, University of Southern California, Los Angeles, CA 90045.

*Address reprint requests to: F.G.S., 7511 McConnell Ave., Los Angeles, CA 90045. E-mail: MRIsafety.com

Received February 8, 2000; Accepted March 18, 2000.

Table 1
List of Heart Valve Prostheses Evaluated for MR Safety at 1.5 T

| No | Prosthesis, manufacturer ^a | Type | Site | Model | Size (mm) | Materials | Additional materials |
|----|--|------------------|--------|-----------------------|-----------|---|---|
| 1 | AorTech | Single leaflet | Aortic | 3800 | 23 | Pyrolitic carbon | Grade A-70 titanium with knitted Teflon |
| 2 | AorTech Aortech Ltd., Caledonian House, Phoenix Crescent, Strathclyde Strathclyde, UK | Single leaflet | Mitral | 4800 | 25 | | |
| 3 | Beall Coratomic Inc., Indianapolis, IN | Caged disc | Mitral | Unknown | 29 | Pyrolitic carbon | Pyrolitic carbon with Dacron |
| 4 | Biocor St. Jude Medical Inc., St. Paul, MN | Animal tissue | Aortic | H3636 | 23 | Porcine tissue | Celon with Dacron |
| 5 | BS Pyrolitic Carbon Conical Disc | Single leaflet | Mitral | MBUP | 21 | Pyrolitic carbon | Chromium cobalt alloy with Teflon |
| 6 | BS Pyrolitic Carbon Conical Disc Pfizer, Inc., Cincinnati, OH | Single leaflet | Mitral | MBRP | 21 | | |
| 7 | BS Monostrut | Single leaflet | Mitral | MBUM | 25 | Pyrolitic carbon | Chromium cobalt alloy with Teflon |
| 8 | BS Monostrut | Single leaflet | Aortic | ABMS | 17 | | |
| 9 | BS Shiley Monostrut Pfizer, Inc., Cincinnati, OH | Single leaflet | Mitral | MBRMS | 23 | | |
| 10 | Jyros | Bileaflet | Mitral | J1M | 30 | Pyrolitic carbon | Carbon |
| 11 | Jyros | Bileaflet | Aortic | J1A | 26 | Pyrolitic carbon Impregnated with boron carbide | |
| 12 | Axion Medical Ltd. Hancock Pericardial | Animal tissue | Mitral | T410 | 25 | Bovine tissue | Haynes alloy with polyester fabric |
| 13 | Medtronic Inc., Minneapolis, MN Intact | Animal tissue | Aortic | A805 | 19 | Porcine tissue | Acetyl copolymer covered with Dacron polyester fabric |
| 14 | Intact | Animal tissue | Mitral | M705 | 25 | | |
| 15 | Medtronic Inc., Minneapolis, MN Liotta | Animal tissue | Aortic | MA783 | 23 | Porcine tissue | Acetatal resin frame; Delrin, low profile stent with Dacron cloth |
| 16 | St. Jude Medical Inc., St. Paul, MN Mitroflow | Animal tissue | Aortic | 11A | 25 | Bovine tissue | Delrin (polyacetal homopolymer), Dacron fabric with flexible tungsten loaded silicone |
| 17 | Mitroflow | Animal tissue | Mitral | 11M | 29 | | |
| 18 | Mitroflow | Animal tissue | Aortic | 14A | 25 | | |
| 19 | Sulzer CarboMedics, UK Smelloff Cutter | Caged ball | Aortic | Unknown | 21 | Silicone rubber | Titanium with bar metal with polyester |
| 20 | Sorin Biomedica, Italy Sorin Pericarbon (stented) | Animal tissue | Mitral | SM | 33 | Bovine tissue | Pyrolitic carbon coated with Carbofilm |
| 21 | Sorin Biomedica, Italy Tascon Medtronic Inc., Minneapolis, MN | Animal tissue | Aortic | Unknown | Unknown | Porcine tissue | Elgiloy with polyester |
| 22 | Wessex | Animal tissue | Aortic | WAV10 | 31 | Porcine tissue | Acetal polymer with cloth reinforced with silicone rubber |
| 23 | Wessex | Animal tissue | Mitral | WMV20 | 25 | | |
| 24 | Sorin Biomedica, Italy Xenofic | Animal tissue | Aortic | AP80 | 23 | Bovine tissue | Teflon with stainless steel marker |
| 25 | Unknown ATS Medical Open Pivot ATS Medical Inc., Minneapolis, MN | Bileaflet | Mitral | 500DM29 | 29 | Pyrolytic carbon | Teflon |
| 26 | ATS Medical Open Pivot ATS Medical Inc., Minneapolis, MN | Bileaflet | Aortic | 501DA18 | 18 | Pyrolytic carbon | Teflon |
| 27 | SJM Reagent Valve | Bileaflet | Aortic | 25AGN- 751- IDE | 25 | Polyester | |
| 28 | Mechanical Heart Valve St. Jude Medical Inc., St. Paul, MN St. Jude Medical Mechanical Heart valve St. Jude Medical Inc., St. Paul, MN | Bileaflet | Aortic | 25AJ- 501 | 25 | Polyester | |

Table 1
(Continued)

| No | Prosthesis, manufacturer ^a | Type | Site | Model | Size (mm) | Materials | Additional materials |
|----|--|---------------|--------|--------------------|-----------|------------------|-------------------------|
| 29 | Toronto SPV Valve St. Jude Medical Inc., St. Paul, MN | Animal tissue | Aortic | SPA- 101- 25 | 25 | Porcine tissue | |
| 30 | Duraflac Unknown | Human tissue | Aortic | AD | 33 | Human tissue | |
| 31 | Duraflac Unknown | Human tissue | Mitral | MD | N/A | Human tissue | |
| 32 | Sorin Allcarbon, AS Sorin Biomedica Cardio S.p.A., Saluggia, Italy | Bileaflet | Mitral | MTR- 29AS | 29 | Pyrolytic carbon | Teflon-coated Carbofilm |

^aBS = Bjork Shiley.

spatial gradient of the magnetic field was previously determined to be at a maximum (35 cm inside the bore of the MR magnet) to assess the magnetic field translational attraction with regard to an extreme condition, as previously described (21–25,33). The highest spatial gradient for the shielded 1.5-T MR system used for this evaluation is 450 gauss/cm and occurs at an off-axis position in the bore of the MR system, according to the survey conducted on the magnetic field using a gauss meter (21–25,33).

Further assessment of magnetic field interactions was conducted to determine qualitatively the presence of magnetic field-induced torque (16,17,24,33). Each heart valve was positioned in the center of the MR system, where the effect of torque from the 1.5-T static magnetic field is known to be the greatest. The heart valve was directly observed for any type of possible movement with respect to alignment or rotation to the magnetic field. The observation process was facilitated by having the investigator inside the bore of the magnet during the test procedure. The heart valve was rotated in 45° increments during this test procedure to observe the effects of torque. This process was repeated to encompass a full 360° rotation of positions for the heart valve prostheses.

The following qualitative scale of torque was applied to the results, as previously described (21,22,23,24): 0, no torque; +1, mild torque (the device changed orientation slightly but did not align to the magnetic field); +2, moderate torque (the device aligned gradually to the magnetic field); +3, strong torque (the device showed rapid and forceful alignment to the magnetic field); and +4, very strong torque (the device showed very rapid and very forceful alignment to the magnetic field).

Assessment of Heating

Each heart valve prosthesis was assessed for heating during MRI that was conducted using a relatively high level of exposure to RF radiation. A 1.5-T/64-MHz MR system (General Electric Medical Systems, Milwaukee, WI) was used for this experiment along with the body coil to send and receive RF energy. An experiment using a relatively high level of exposure to RF power was conducted with the heart valve prosthesis positioned in a special phantom filled with a semisolid gel (35).

In order to utilize a relatively high exposure to radio frequency (RF) power, the following pulse sequence was used: T1-weighted spin-echo, as follows: total imaging time 15 minutes; axial plane; TR/TE 134/25 msec; field of view (FOV) 48 cm; imaging matrix 256 × 128; section thickness 20 mm; number of section locations 5; number of excitations 54; number of echos 4; phasing direction anterior to posterior; transmitter gain 200. This pulse sequence produced a whole-body averaged specific absorption rate (SAR) of 1.1 W/kg. This level of exposure to RF energy exceeds that typically used for MR imaging of patients and is similar to that used by other researchers to examine heating for implants in association with MRI (23,24,34). Since there is no blood flow associated with this experimental procedure, it further simulates an extreme condition for MRI-related heating.

A plastic phantom was used that was 28 cm deep, 54 cm long, and 30 cm wide (to approximate the size of the human thorax). This phantom was filled with a semi-solid gel to provide a highly conductive medium to surround the heart valve prosthesis for the heating experiment. A plastic frame (ie, with holes 5 mm spaced 5 mm apart) was used to position the heart valve prosthesis within the phantom such that it was placed in a position close to the bore of the MR system (where RF heating would be greatest).

The semisolid gel was prepared to simulate human tissue. This was accomplished using a gelling agent [hydroxyethyl-cellulose (HEC)] in an aqueous solution (91.58% water) along with 0.12% NaCl to create a dielectric constant of approximately 80 and a conductivity of 0.8 S/m at 64 MHz. This is an acceptable dielectric constant and an acceptable conductivity for evaluation of MRI-related heating of an implant (35).

A Luxtron model 3100 fluoroptic thermometry system (Santa Clara, CA) was used to measure temperatures before and during MRI. The thermometry probe was placed on the exposed metallic portion of the heart valve prosthesis (ie, for those with exposed metal) or the ring portion of the heart valve prosthesis (ie, for the valves that were predominantly tissue). Additionally, a thermometry probe was placed in the gel at the opposite side of the phantom to record a reference temperature (ie, remote from the heart valve prosthesis).

The room and bore temperatures were stable and recorded to be 21.1°C for the heating experiments. The MR system fan was not on during the procedures. Baseline temperatures were recorded for 5 minutes at 1-minute intervals, after which MRI was performed for 15 minutes with temperatures recorded at 20-second intervals. The highest temperature changes are reported for the heart valve prostheses and the reference temperatures.

Assessment of Artifacts

While artifacts are not a primary safety concern for implants, the presence of an artifact is typically of interest to MR health care workers. Thus, artifacts associated with MRI were determined for these heart valve prostheses. A rectangular gel-filled phantom was used for this test. The T1 and T2 values for this gel were similar to those for muscle tissue. MRI was performed using a 1.5-T MR system and a send-receive body coil. The following pulse sequences were used:

1. Gradient-recalled echo in the steady-state pulse sequence; TR/TE 100/15 msec; flip angle 30°; bandwidth 16 kHz; matrix size 256 × 256; section thickness 10 mm; FOV 38 cm; number of excitations 2.
2. T1-weighted spin-echo pulse sequence; TR/TE 300/20 msec; bandwidth 16 kHz; matrix size 256 × 256; section thickness 10 mm; FOV 38 cm; number of excitations 2.0.

A plastic frame (ie, with holes 5 mm spaced 5 mm apart) was used to position the heart valve prostheses 12 at a time (ie, numbers 1–12 were scanned, and then numbers 13–24). The imaging planes were oriented at a parallel position relative to the centermost part of the heart valves. The frequency-encoding direction was parallel to the plane of imaging. Note that MR imaging artifacts that result from other pulse sequences or from other positions of the imaging plane relative to the heart valves or with regard to the particular orientation of the clips to the main magnetic field of the MR system may be slightly more or less than that observed under the experimental conditions used in the above-indicated test for artifact assessment (14,15,18,19,21–24).

Furthermore, the artifact size will vary depending on the TE used for the fast multiplanar spoiled gradient-echo pulse sequence (ie, the artifact size is greater for a higher TE). Nevertheless, the specific MR technique used to assess artifacts is the same as that used before and published in the peer-reviewed literature (14–16,18,19,21–24).

Artifact size was graded according to the following scheme: neg., no artifact; +1, artifact less than the size of the device; +2, artifact same as the size of the device; +3, artifact slightly larger than the size of the device; +4, artifact larger than twice the size of the device. This particular technique of artifact assessment has been used in several prior publications and therefore serves as an appropriate comparison (14–16,18,19). All image display parameters (ie, window and level settings, magnification, etc.) were carefully selected and used in a consistent manner to facilitate a valid determination of artifact size.

RESULTS

A summary of the test results for ferromagnetism, heating, and artifacts associated with heart valve prostheses is presented in Table 2. The deflection angles for these 32 different heart valve prostheses exposed to the 1.5-T MR system ranged from 0 to 5°. The torque for the heart valve prostheses ranged from 0 to +2 (Table 2). These findings suggest that the type of materials used for these prostheses were either nonferromagnetic or only weakly ferromagnetic relative to the 1.5-T MR environment.

In the assessment of RF heating associated with MRI, the highest temperature changes recorded for the 32 different valve prostheses ranged +0.5 to +0.8°C. The highest reference temperature changes ranged from +0.4 to +0.5°C.

The sizes of the artifacts ranged from mild (+2) to severe (+4) and appeared as localized signal voids, easily recognizable on the image. In general, the gradient-echo pulse sequence produced a larger artifact than the T1-weighted pulse sequence for these heart valve prostheses. Additionally, artifacts were directly proportional to the amount of metal present for a given heart valve prosthesis. Figure 1 shows MR images that display representative artifact findings for the various heart valve prostheses using the gradient-echo pulse sequence.

DISCUSSION

Despite its relatively short history, there has been a rapid increase in the development of MRI techniques as well as substantial advances in clinical applications. As a consequence, there has been a proliferation in MRI procedures together with a concomitant increase in the number of patients undergoing MRI. MRI is an important diagnostic tool for virtually every clinical speciality.

In general, MRI is considered one of the safest non-invasive imaging modalities (5,6,8). MR health care workers are nevertheless concerned about the possible interaction between heart valve prostheses and the magnetic field of the MR system. Of particular concern are the possible effects of magnet-related translation and torque interactions on the prosthesis (1,2,6,7). Notably, in this study, few heart valve prostheses displayed measurable degrees of deflection and/or torque (Table 1). Those that did are considered to have minor magnetic field interactions relative to the force exerted by the beating heart (26,27,29).

The deflection angles measured for the heart valve prostheses ranged from 0 to 5°. According to the American Society for Testing and Materials (ASTM), the operational definition of a nonferromagnetic implant (the ASTM document actually referred to an aneurysm clip) is met if the deflection angle is less than 45° (32). Accordingly, these heart valve prostheses would be deemed safe for individuals in a 1.5-T or less MR environment.

While the torque ranged from 0 to +2 (ie, moderate torque, the device aligned gradually to the magnetic field), these qualitative findings are not believed to present a hazard or risk for these heart valve prostheses. Moreover, during in the in vivo application of these heart valve prostheses, the implants are maintained in

Table 2
Results of MR Safety Tests for Prosthetic Heart Valves

| No | Prosthetic heart valve ^a | Deflection angle (°) | Torque | Temp. change (°) | Artifact grade | |
|----|---|----------------------|--------|------------------|----------------|-----|
| | | | | | T1-SE | GRE |
| 1 | AorTech | 0 | +1 | 0.6 | +2 | +3 |
| 2 | AorTech | 0 | +1 | 0.6 | +2 | +3 |
| 3 | Beall | 0 | +1 | 0.6 | +3 | +4 |
| 4 | Biocor | 0 | 0 | 0.5 | +2 | +2 |
| 5 | BS Pyrolytic Carbon Conical Disc | 0 | 0 | 0.5 | +3 | +3 |
| 6 | BS Pyrolytic Carbon Conical Disc | 0.5 | +1 | 0.7 | +3 | +4 |
| 7 | BS Monostrut | 0.5 | +1 | 0.6 | +3 | +4 |
| 8 | BS Monostrut | 0 | 0 | 0.5 | +3 | +3 |
| 9 | BS Monostrut | 0 | 0 | 0.5 | +3 | +3 |
| 10 | Jyros | 0 | 0 | 0.6 | +4 | +4 |
| 11 | Jyros | 0 | 0 | 0.5 | +3 | +3 |
| 12 | Hancock Pericardial | 0 | 0 | 0.6 | +2 | +3 |
| 13 | Intact | 0 | 0 | 0.5 | +3 | +4 |
| 14 | Intact | 0 | 0 | 0.6 | +2 | +2 |
| 15 | Liotta | 0 | 0 | 0.5 | +2 | +2 |
| 16 | Mitroflow | 0 | 0 | 0.5 | +3 | +4 |
| 17 | Mitroflow | 0 | 0 | 0.5 | +2 | +2 |
| 18 | Mitroflow | 0 | 0 | 0.5 | +3 | +3 |
| 10 | Smeloff Cutter | 3.0 | +2 | 0.7 | +2 | +3 |
| 20 | Sorin Pericarbon (stented) | 0 | 0 | 0.5 | +2 | +3 |
| 21 | Tascon | 0 | 0 | 0.6 | +2 | +2 |
| 22 | Wessex | 0 | 0 | 0.5 | +2 | +2 |
| 23 | Wessex | 0 | 0 | 0.5 | +2 | +2 |
| 24 | Xenofic | 0 | 0 | 0.5 | +2 | +2 |
| 25 | ATS Medical Open Pivot, 29 | 0 | +1 | 0.7 | +3 | +4 |
| 26 | ATS Medical Open Pivot, 18 | 0 | +1 | 0.5 | +3 | +4 |
| 27 | SJM Reagent Valve | 0 | +1 | 0.7 | +2 | +4 |
| 28 | St. Jude Medical Mechanical Heart Valve | 0 | +1 | 0.6 | +2 | +4 |
| 29 | Toronto SPV Valve | 0 | 0 | 0.5 | +2 | +2 |
| 30 | Duraflac, Aortic | 5.0 | +2 | 0.8 | +3 | +4 |
| 31 | Duraflac, Mitral | 2.0 | +2 | 0.7 | +3 | +4 |
| 32 | Sorin Allcarbon, AS | 0 | +1 | 0.6 | +3 | +4 |

^aBS = Bjork Shiley.

position by multiple sutures and eventual tissue in growth. These important aspects must be carefully considered as they serve as retentive forces to maintain the heart valve prostheses in place during exposure to the MR environment (ie, even for the heart valve prostheses that displayed +2 torque).

The overall findings for magnetic field interactions are similar to those of other investigators that assessed magnetic qualities of heart valve prostheses in association with MR systems (2,26–30). Thus, a patient with any heart valve prosthesis listed in Table 1 undergoing an MRI procedure using an MR system operating at 1.5 T or less would not be at risk with regard to movement or dislodgement of the implant.

Additional concerns about the safety of heart valve prostheses and other implants relate to the potential heating of the implant. Temperature elevations during MRI procedures have been studied using ex vivo techniques for many different types of bioimplants, including heart valve prostheses (4,9,11,14,16,19–24,29,33–36). The temperature elevations exhibited in this study, although only minor, are nonetheless marginally higher than those recorded by other researchers evaluating the effects of RF heating in heart valve prostheses (26,28,29). This may be explained by the fact that the

experimental procedure utilized a semisolid gel while the other studies typically used a saline bath. Nevertheless, these marginally higher temperature increases during MRI are still believed to be safe for patients undergoing MR procedures, in consideration of the exposure to the relatively high level of RF energy (ie, a whole-body averaged SAR of 1.1 W/kg).

While MRI related artifacts are not a primary safety issue for implants, the presence of an artifact may affect the diagnostic imaging quality of an MRI examination if the area of interest is in the exact same position where the heart valve prosthesis is located. Artifacts were characterized for the 32 different heart valve prostheses using a previously published grading scheme. While there are obviously more sophisticated techniques to assess artifacts for implants, this was not a primary objective of the present study, nor do these techniques tend to provide clinically relevant data. Nevertheless, the artifact findings are deemed useful using the qualitative grading technique insofar as it can readily be appreciated that certain heart valve prostheses (eg, heart valve prostheses numbers 3, 6, 7, 10, 13, and 16) would probably impair the diagnostic aspects of the MRI examination if in the area of interest. However, artifact size may be minimized for metallic implants with the

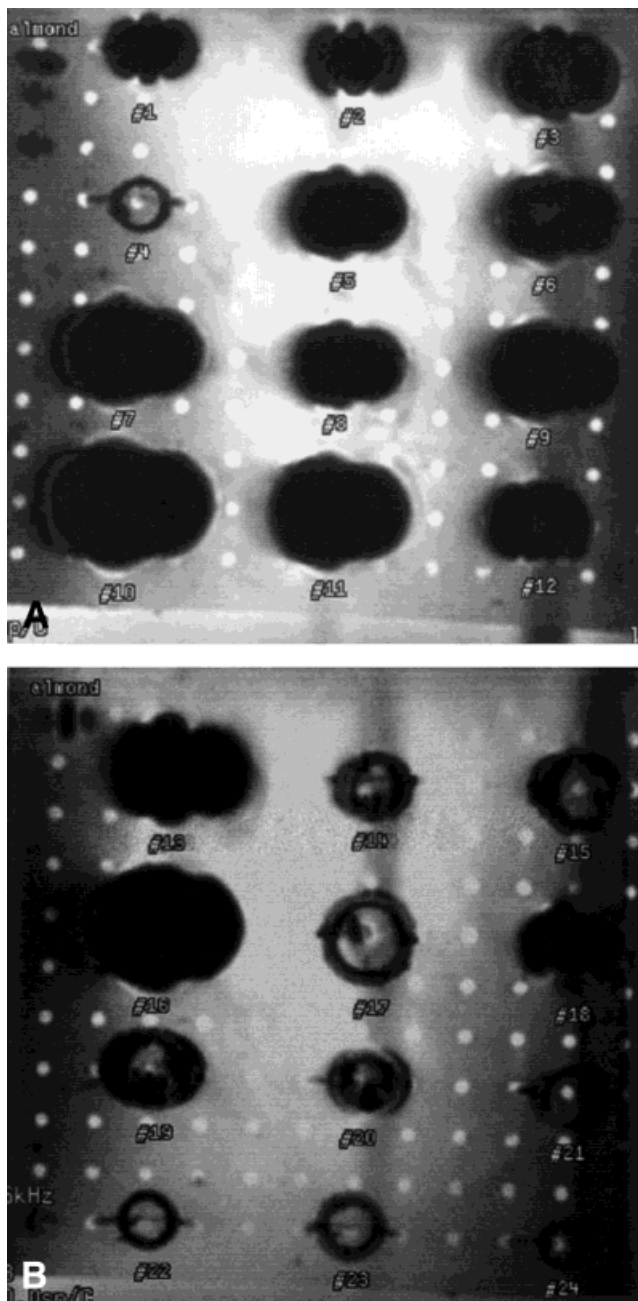


Figure 1. MR images of heart valve prostheses obtained using a gradient-echo pulse sequence (coronal plane, TR/TE 100/15 msec, flip angle, 30°; FOV, 38 cm) showing examples of artifacts. Note the differences in artifacts size, primarily related to the amount of metal in the heart valve prosthesis (Note: an average-sized almond was placed in the left corner as a reference object). **A:** Heart valve prostheses numbers 1–12. **B:** Heart valve prostheses numbers 13–24. The numbers correspond to the scheme in Table 1 (note that MR images are not provided for valves 25–32).

selection of imaging parameters (eg, use of a fast spin-echo in comparison with a conventional spin-echo pulse sequence) and by other means.

SUMMARY AND CONCLUSIONS

MRI safety was determined for 32 different heart valve prostheses using ex vivo test procedures in association

with a 1.5-T MR system. All prosthetic heart valves were tested for magnetic field interactions, heating, and artifacts. The data revealed only minor magnetic field interactions with temperature changes that were substantially below that known to pose a hazard to human subjects. Artifacts were characterized as mild to severe in size.

Based on this information, these heart valve prostheses should not present a hazard with respect to movement or dislodgement in MRI environments of 1.5 T or less. Additionally, RF energy-induced heating associated with a whole-body averaged SAR of 1.1 W/kg will not pose a risk to a patient with one of these heart valve prostheses. Accordingly, these heart valve prostheses should be considered “MR safe” according to the specific conditions used for testing.¹

ACKNOWLEDGMENTS

The authors thank Dr. Pat Lawford, Department of Medical Physics and Clinical Engineering, Royal Hallamshire Hospital, Sheffield, for her encouragement and invaluable input into this project.

REFERENCES

1. New PFJ, Rosen BR, Brady TJ, et al. Potential hazards and artifacts of ferromagnetic and non-ferromagnetic surgical and dental devices in nuclear magnetic resonance imaging. *Radiology* 1983;147:139–148.
2. Shellock FG, Cruess JV. High-field MR imaging of metallic implants: an ex vivo evaluation of deflection forces. *AJR* 1988;151:389–392.
3. Malott JC. Hazards of ferrous materials in MRI: a case report. *Radiol Technol* 1997;53:233–235.
4. Buchli Boesiger P, Meier D. Heating effects of metallic implants by MRI examinations. *Magn Reson Med* 1988;7:255–261.
5. Kanal E, Shellock FG, Talagala L. Safety considerations in MR imaging. *Radiology* 1990;176:593–606.
6. Shellock FG, Kanal E. *Magnetic resonance: bioeffects, safety, and patient management*. New York: Lippincott, Williams & Wilkins 1996.
7. Bromage PR, Kozic Z. Magnetic resonance imaging implications of metal-reinforced spinal microcatheters. *J Clin Anesth* 1991;3:382–385.
8. Shellock FG. *Pocket guide to MR procedures and metallic implants: update 2000*. Philadelphia: Lippincott, Williams & Wilkins; 2000.
9. Davis PL, Crooks L, Arakawa M, et al. Potential hazards in NMR imaging: heating effects of changing magnetic fields and RF fields on small metallic implants. *AJR* 1991;173:857–860.
10. Teitelbaum GP, Raney M, Carvlin MJ, et al. Evaluation of ferromagnetism and magnetic resonance imaging artifacts of the Strecker tantalum vascular stent. *Cardiovasc Intervent Radiol* 1989;12:125–127.
11. Shellock FG, Nogueira M, Morisoli M. MRI imaging and vascular access ports: ex vivo evaluation of ferromagnetism, heating, and artifacts at 1.5 T. *J Magn Reson Imaging* 1995;4:481–484.
12. Kotsakis A, Tan KH, Jackson G. Is MRI a safe procedure in patients with coronary stents in situ? *Int J Cardiovasc Radiol* 1997;51:34.
13. Randall PA, Kohman LJ, Scalzetti EM, Szeverenyi NM, Panicek DM. Magnetic resonance imaging of prosthetic cardiac valves in vitro and in vivo. *Am J Cardiol* 1988;62:973–976.
14. Shellock FG, Shellock VJ. Metallic marking clips used after stereotactic breast biopsy: ex vivo testing of ferromagnetism, heating, and artifacts associated with MRI. *AJR* 1999;172:1417–1419.

¹The results of this study will be included on the web site www.MRIsafety.com, which has a comprehensive listing of implants, devices, and objects that have undergone testing for MRI safety. MRIsafety.com provides crucial information to healthcare providers and patients seeking answers to questions on MRI safety-related topics. In addition, the latest information on screening patients with implants, materials, and medical devices is provided. MRIsafety.com was developed and is maintained by Frank G. Shellock, PhD.

15. Shellock FG, Meeks T. Ex vivo evaluation of ferromagnetism and artifacts for implantable vascular access ports exposed to a 1.5 T MR scanner. *J Magn Reson Imaging* 1991;1:243-246.
16. Shellock FG, Shellock VJ. Cardiovascular catheters and accessories: ex vivo testing of ferromagnetism, heating, and artifacts associated with MRI. *J Magn Reson Imaging* 1998;8:1338-1342.
17. Nogueira M, Shellock FG. Otologic bioimplants: ex vivo assessment of ferromagnetism and artifacts at 1.5 Tesla. *AJR* 1993;163:1472-1473.
18. Shellock FG, Morisoli SM. Ex vivo evaluation of ferromagnetism and artifacts for cardiac occluders exposed to a 1.5 Tesla MR system. *J Magn Reson Imaging* 1994;4:213-215.
19. Shellock FG, Nogueira M, Morisoli M. MRI imaging and vascular access ports: ex vivo evaluation of ferromagnetism, heating, and artifacts at 1.5 T. *J Magn Reson Imaging* 1995;4:481-484.
20. Shellock FG, Shellock VJ. Ceramic surgical instruments: evaluation of MR-compatibility at 1.5 Tesla. *J Magn Reson Imaging* 1996;6:954-956.
21. Shellock FG, Shellock VJ. MR-compatibility evaluation of the Spetzler titanium aneurysm clip. *Radiology* 1998;206:838-841.
22. Shellock FG, Shellock VJ. Evaluation of cranial flap fixation clamps for compatibility with MR imaging. *Radiology* 1998;207:822-825.
23. Shellock FG. MR-compatibility of an endoscope designed for use in interventional MRI procedures. *AJR* 1998;171:1297-1300.
24. Shellock FG, Shellock VJ. Metallic stents: evaluation of MR imaging safety. *AJR* 1999;173:543-547.
25. Kanal E, Shellock FG. Aneurysm clips: effects of long-term and multiple exposures to a 1.5 Tesla MR system. *Radiology* 1999;210:563-565.
26. Soulen RL, Budinger TF, Higgins CB. Magnetic resonance imaging of prosthetic heart valves. *Radiology* 1985;154:705-707.
27. Soulen RL. Magnetic resonance imaging of prosthetic heart valves. *Radiology (letter)* 1986;158:279.
28. Randall PA, Kohman LJ, Scalzetti EM, Szeverenyi NM, Panicek DM. Magnetic resonance imaging of prosthetic cardiac valves in vitro and in vivo. *Am J Cardiol* 1988;62:973-976.
29. Shellock FG, Morisoli SM. Ex vivo evaluation of ferromagnetism, heating, and artifacts for heart valve prostheses exposed to a 1.5 Tesla MR system. *J Magn Reson Imaging* 1994;4:756-758.
30. Di Cesare E, Enric RM, Paparoni S, et al. Low-field magnetic resonance imaging in the evaluation of mechanical and biological heart valve function. *Eur J Radiology* 1995;20:224-228.
31. Edwards MB. Prosthetic heart valves implanted in the United Kingdom: 1986 to 1997. London: UK Heart Valve Registry.
32. American Society for Testing and Materials. Standard specification for the requirements and disclosure of self-closing aneurysm clips. In: *Annual Book of ASTM Standards*, 1994.
33. Shellock FG, Detrick MS, Brant-Zawadski M. MR-compatibility of Guglielmi detachable coils. *Radiology* 1997;203:568-570.
34. Chou C-K, McDougall JA, Chan KW. RF heating of implanted spinal fusion stimulator during magnetic resonance imaging. *IEEE Trans Biomed Eng* 1997;44:367-372.
35. Nyehnuis JA, Kildishev AV, Bourland JD, Foster KS, Graber G. Heating near implanted medical devices by MRI RF-magnetic field. *IEEE Trans* 1999;35:4133-4135.
36. Shellock FG, Hatfield M, Simon BJ, et al. Implantable spinal fusion stimulator: assessment of MRI safety. *J Magn Reson Imaging* (in press).